Fracture Mechanics of Concrete and Concrete Structures -
Recent Advances in Fracture Mechanics of Concrete - B. H. Oh, et al.(eds)

A mixed mode model for fracture in concrete

L. O. Nielsen, J. F. Mougaard, J. S. Jacobsen & P. N. Poulsen
Technical University of Denmark, Lyngby, Denmark

ABSTRACT: In the present work a new mixed mode fracture model for concrete is developed. The model is based on elastoplasticity with damage, and consists of a friction and a cohesion part. The cohesion part includes damage, which is capable of exhausting the cohesion as function of the crack opening in an irreversible process. The friction part includes deformation state dependency, which makes the model capable of representing decreasing friction when the crack opens and increasing friction when the crack closes in a reversible way. The performance of the model is compared with results from the literature.

1 INTRODUCTION

For accurate modelling of cracks in concrete a realistic constitutive model is needed. A well documented constitutive model concerning crack initiation and Mode I behaviour in concrete is the fictitious model by Hillerborg (1989). However, the sliding in the crack may also be essential, e.g. in shear cracks and in the debonding process around a reinforcement bar. A softening elastoplastic model for the opening-sliding mixed mode has been proposed by Carol (1997), but lacks reversible friction behaviour.

The opening-sliding deformation in a crack weakens the cohesion in the material. This non-reversible process may be modelled with elastoplastic damage. When the cohesion in the crack is exhausted, frictional strength capacity still exist between the crack faces if these have not been moved to far away from each other. Moreover the frictional strength capacity is increased if the crack faces are moved closer to each other. So the frictional phenomenon is of reversible type and dependent on the crack deformations. A modelling of this may be based on deformation state dependent plasticity. A friction-cohesion model with this basis is presented in this paper. Somewhat different models without deformation state dependent plasticity are described in Jefferson (1998) and Spada (2009), while Alfano (2006) describes a rather complicated thermodynamic based model. For general survey is referred to Spada (2009) and Alfano (2006).

2 FRICTION-COHESION CONSTITUTIVE MODEL

Below are assumed small strains and we consider the material as a continuum, which initially is isotropic.

We consider a body in which a cohesive crack is formed in a point P of a surface, if the normal stress σ on the cracking surface in P reaches the tension strength f_t of the material, i.e. the crack initiation criterion is

$$\sigma_1 = f_t \tag{1}$$

where σ_1 is the largest principal stress in P. In this paper is described a constitutive model for the further evolution of the crack. The model is relevant for modeling concrete structures containing e.g. cohesive cracks and yield lines.

The crack, which is distributed somehow over a narrow crack process zone, is here modelled as a displacement discontinuity between the two faces of the cracking surface. In a point P on the discontinuity surface the normal stress is σ and the shear stress is τ with a direction s see Figure 1. The unit normal $\mathbf{n}$ to the discontinuity surface is directed from the – face to the + face. The displacements u_n, u_s are subscripted after their direction and superscripted with their face. The generalized strains in the discontinuity surface is the opening $\Delta u_n = u_n^+ - u_n^-$ perpendicular to the discontinuity surface and the sliding along the discontinuity surface $\Delta u_s = u_s^+ - u_s^-$. Organized in a column matrix the generalized strains $\boldsymbol{\varepsilon}^T = \begin{bmatrix} \Delta u_n & \Delta u_s \end{bmatrix}$, where superscript T on a matrix means transposed. In the following is considered only the plane problem, i.e. τ and Δu_s are fixed to a plane – the figure plane on Figure 1.

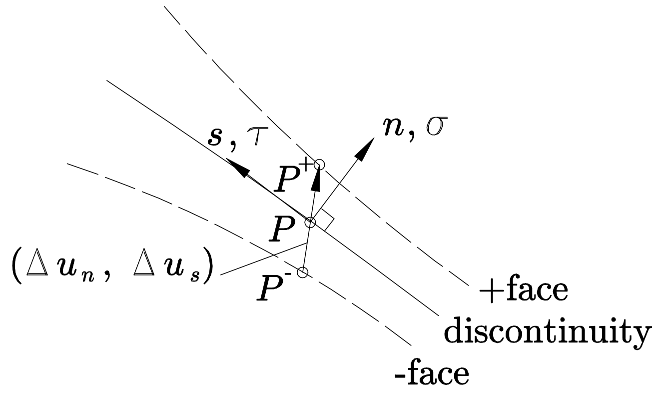

Figure 1. Notation in discontinuity surface. Point P on the discontinuity surface is splitted in two points P^+ on the + face and P^- on the – face.

A classical failure model for the discontinuity surface is the modified Coulomb (mC) model Figure 1, which restricts the stresses in a point of the body to

$$\tau \le c - \mu\sigma \quad \sigma_1 \le f_t \tag{2}$$

where σ_1 is the largest principal stress in the point considered and the material parameters comprise the cohesion c, the coefficient of internal friction μ and the tension strength f_t. Closely related to experiments suitable independent material parameters are μ or the friction angle φ ($\mu = \tan\varphi$), f_t and the compression strength f_c, while c is determined from these and Equation 2. The mC model indicates a strength contribution from the cohesion in the material and a contribution from the friction in the material. This indication is followed in the friction-cohesion model described below.

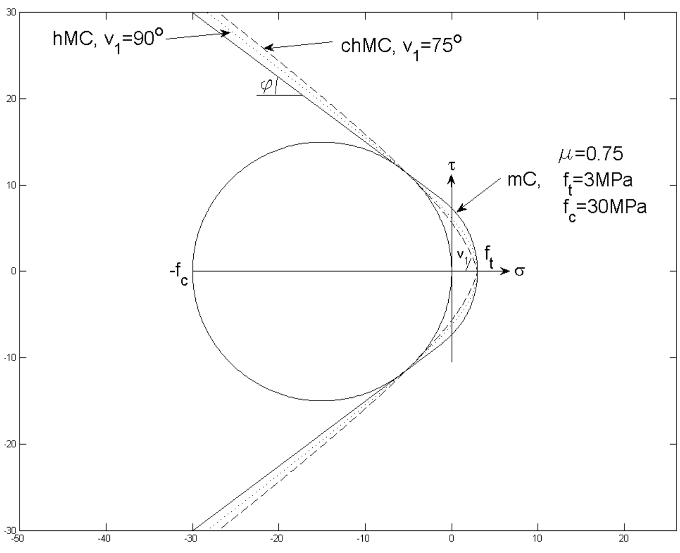

Figure 2. Yield surfaces based on the mC, hMC and chMC models together with Mohr's circle for uniaxial compression.

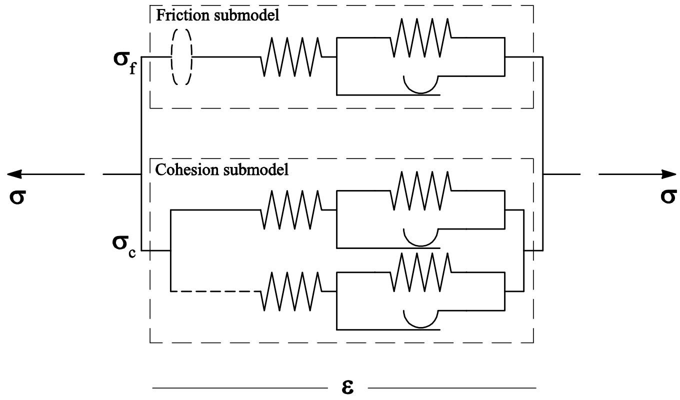

Figure 3. Friction-cohesion model. A dashed line (----) indicates a weakening in tension.

The main features of the friction-cohesion model are shown on Figure 3. The model consists of a friction submodel (subscript f) in parallel with a cohesion submodel (subscript c), i.e. the total stresses ($\boldsymbol{\sigma}^T = \begin{bmatrix}\sigma & \tau\end{bmatrix}$) are the sum of the stresses in the friction submodel and the stresses in the cohesion submodel

$$\boldsymbol{\sigma} = \begin{bmatrix}\sigma \\ \tau\end{bmatrix} = \begin{bmatrix}\sigma_f \\ \tau_f\end{bmatrix} + \begin{bmatrix}\sigma_c \\ \tau_c\end{bmatrix} \tag{3}$$

The submodels are elastic, perfectly plastic materials with reversible deformation state dependence in the friction submodel to model reduced shear resistance with crack opening and damage in the cohesion submodel to model damage of the cohesion with crack deformation.

While the mC failure criterion in Equation 2 is successful as perfect plasticity model for the concrete in concrete structures in connection with limit analysis see Nielsen (1999), it seems insufficient as basis for a more detailed description of the stress-strain behaviour in a displacement discontinuity and its evolution. A useful basis for the plasticity parts of the friction-cohesion model seems to be a hyperbolic Mohr-Coulomb yield condition with a controllable cusp (called chMC with cusp and hMC without cusp) in the pure tension point on the σ-axis. The yield function $f(\sigma,\tau)$ is determined by

$$f(\sigma,\tau) = \tau^2 + \beta|\tau| - (c-\mu\sigma)^2 + (c-\mu f_t)^2$$
$$f_t \le \frac{c}{\mu} \tag{4}$$

where the new material parameter β controls the opening angle $2v_1$ of the cusp, see Figure 2. For $\beta = 0$ the cusp vanishes. For large compression the relative deviation from mC becomes small. Closely related to experiments suitable independent material parameters are μ or φ, f_t, f_c and v_1, while c and β are determined from these and Equation 4.

As non-hardening seems to suffice, these parameters can be considered as constants for a given material. The chMC and the hMC yield surfaces $f(\sigma,\tau)=0$ are shown on Figure 2. Obviously the shear capacity is essentially reduced in tension and in slight compression compared with the modified Coulomb model.

3 COHESION SUBMODEL

The cohesion submodel is an elastic, perfectly plastic material with damage. It is introduced in uniaxial tension, because the friction submodel of the full model then is inactive. The cohesion submodel should be realistic in tension, in tension and shear and in slight compression and shear. Otherwise the friction submodel will dominate.

The permanent deformation connected to elastoplasticity Figure 4a and the stiffness degradation connected to damage Figure 4b are basic properties modeling concrete in uniaxial tension. Therefore it is obvious to combine elastoplasticity with damage in a model for concrete as indicated in the cohesion submodel on Figure 3. Moreover, as the intention is to model frictional sliding only in the friction submodel, an associated flow rule is a natural choice for the elastoplasticity in the cohesion submodel.

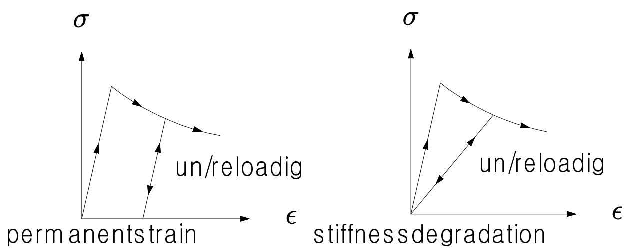

Figure 4. Typical stress-strain behaviour a) Elastoplasticity b) Damage.

3.1 *Elastoplasticity with Damage*

In order to be able to specify the cohesion submodel, the applied version of elastoplasticity with damage is stated. For computational purposes is needed the incremental constitutive relation

$$d\boldsymbol{\sigma}=\mathbf{D}^{epd}d\boldsymbol{\varepsilon} \tag{5}$$

where $\mathbf{D}^{epd}$ is the tangential material stiffness matrix for elastoplasticity with damage.

Damage is described by the damage parameter $\omega, 0\le\omega\le 1$ or the damage history parameter κ^d. Then there must exist a relation between the two quantities

$$\omega=g^d(\kappa^d) \tag{6}$$

where g^d is the damage function. The relation

$$\boldsymbol{\sigma}=(1-\omega)\bar{\boldsymbol{\sigma}} \tag{7}$$

where $\boldsymbol{\sigma}$ represents the nominal stresses and $\bar{\boldsymbol{\sigma}}$ represent the effective stresses, see Figure 3, where ω is given a clear geometrical interpretation as the relative damaged area in a section in the material.

Both the elastic and the elastoplastic part of the model on Figure 3 concerns the effective stresses $\bar{\boldsymbol{\sigma}}$. Then

$$d\bar{\boldsymbol{\sigma}}=\mathbf{D}d\boldsymbol{\varepsilon}^e \quad d\bar{\boldsymbol{\sigma}}=\mathbf{D}^{ep}d\boldsymbol{\varepsilon} \tag{8}$$

where $\mathbf{D}$ is the linear elastic material stiffness matrix and $\mathbf{D}^{ep}$ the tangential material stiffness matrix for elastoplasticity.

Damage occurs when the strain level exceeds previous strain levels. Damage characterized by the total strains $\boldsymbol{\varepsilon}=\boldsymbol{\varepsilon}^e+\boldsymbol{\varepsilon}^p$ is considered here, i.e. the damage loading function f^d is described by

$$f^d=\tilde{\varepsilon}(\boldsymbol{\varepsilon})-\kappa^d \tag{9}$$

where the equivalent strain $\tilde{\varepsilon}$ is some measure of the actual strain state, i.e. it can be expressed by the generalized strains $\boldsymbol{\varepsilon}^T=\begin{bmatrix}\varepsilon_1 & \varepsilon_2 & ...\end{bmatrix}$. The damage loading function and the damage history parameter must satify

$$f^d\le 0 \quad d\kappa^d\ge 0 \quad f^d d\kappa^d=0 \tag{10}$$

The incremental form of Equation 7 is

$$d\boldsymbol{\sigma}=-d\omega\bar{\boldsymbol{\sigma}}+(1-\omega)d\bar{\boldsymbol{\sigma}} \tag{11}$$

Equation 6 gives

$$d\omega=\frac{\partial g^d}{\partial\kappa^d}d\kappa^d$$

Now is considered the active state in regard to damage. Then $f^d=0$ and Equation 9 gives $\tilde{\varepsilon}=\kappa^d$, which is inserted in the equation above, i.e.

$$\begin{aligned} d\omega &= \frac{\partial g^d}{\partial\kappa^d}d\tilde{\varepsilon}=\frac{\partial g^d}{\partial\kappa^d}\left(\frac{\partial\tilde{\varepsilon}}{\partial\varepsilon_1}d\varepsilon_1+\frac{\partial\tilde{\varepsilon}}{\partial\varepsilon_2}d\varepsilon_2+...\right) \\ &= \frac{\partial g^d}{\partial\kappa^d}\begin{bmatrix}\frac{\partial\tilde{\varepsilon}}{\partial\varepsilon_1} & \frac{\partial\tilde{\varepsilon}}{\partial\varepsilon_2} & ...\end{bmatrix}\begin{bmatrix}d\varepsilon_1\\ d\varepsilon_2\\ ...\end{bmatrix}\equiv\frac{\partial g^d}{\partial\kappa^d}\frac{\partial\tilde{\varepsilon}}{\partial\boldsymbol{\varepsilon}}^T d\boldsymbol{\varepsilon} \end{aligned} \tag{12}$$

where last equal sign defines $\dfrac{\partial\tilde{\varepsilon}}{\partial\boldsymbol{\varepsilon}}^T$.

Next Equation 12 and 8 are inserted in Equation 11

$$d\boldsymbol{\sigma} = \left((1-\omega)\mathbf{D}^{ep} - \bar{\boldsymbol{\sigma}} \frac{\partial g^d}{\partial \kappa^d} \frac{\partial \tilde{\varepsilon}^T}{\partial \boldsymbol{\varepsilon}} \right) d\boldsymbol{\varepsilon} \equiv \mathbf{D}^{epd} d\boldsymbol{\varepsilon} \qquad (13)$$

where last equal sign defines $\mathbf{D}^{epd}$ in the active state in regard to damage. In the passive state in regard to damage the $\bar{\boldsymbol{\sigma}}$-term vanish from Equation 13 and as $\mathbf{D}^{ep}$ also can cover the pure elastic state ($\mathbf{D}^{ep} = \mathbf{D}^{e}$), Equation 13 - properly interpreted - covers all state combinations.

3.2 *Details of Cohesion Submodel*

In the cohesion submodel the effective normal stress is $\bar{\sigma}_c$ and the effective shear stress $\bar{\tau}_c$. The elastic behaviour is linear and is described by

$$\begin{bmatrix} d\bar{\sigma}_c \\ d\bar{\tau}_c \end{bmatrix} = \begin{bmatrix} E_c & 0 \\ 0 & G_c \end{bmatrix} \begin{bmatrix} d\Delta u_n^e \\ d\Delta u_s^e \end{bmatrix} \qquad (14)$$

where E_c, G_c are material constants. A realistic value for E_c is set up concentrating the strains ε in the crack process zone in the displacement discontinuity Δu_n in the displacement discontinuity surface. With a process zone of thickness *t*, $\Delta u_n = \varepsilon t$. If the material in the process zone has a Young's modulus $E = 21GPa$ and $t = 35mm$

$$\sigma = E\varepsilon = E\frac{\Delta u_n}{t} = E_c \Delta u_n \Rightarrow E_c = \frac{E}{t} = 600MPa/mm$$

The plasticity is perfect with the hMC yield condition $f_c^p(\bar{\sigma}_c, \bar{\tau}_c)$, see Equation 4, given by

$$f_c^p = \bar{\tau}_c^2 - (c_c - \bar{\sigma}_c \mu_c)^2 + (c_c - f_t \mu_c)^2 \qquad (15)$$

where c_c is the cohesion, μ_c the friction coefficient, f_t the tension strength. Of course, hardening could have been incorporated in these parameters in order to be able to control the balance between permanent deformation and stiffness degradation, but in this case it is not necessary.

The damage is described by the length change measure as equivalent strain

$$\tilde{\varepsilon} = \sqrt{\Delta u_n^2 + \Delta u_s^2} \qquad (16)$$

and the damage function $g^d(\kappa^d)$ Figure 7 is determined by

$$g^d = \begin{cases} 0 & \text{for } \kappa^d \le \Delta u_0 \\ 1 - \exp\left(-\dfrac{\kappa^d - \Delta u_0}{\Delta u_f}\right) & \text{for } \kappa^d \ge \Delta u_0 \end{cases} \qquad (17)$$

with $\Delta u_0 = \frac{f_{t0}}{E_c}$, i.e. in uniaxial tension damage begins together with yield, while the opening scale Δu_f is a material constant.

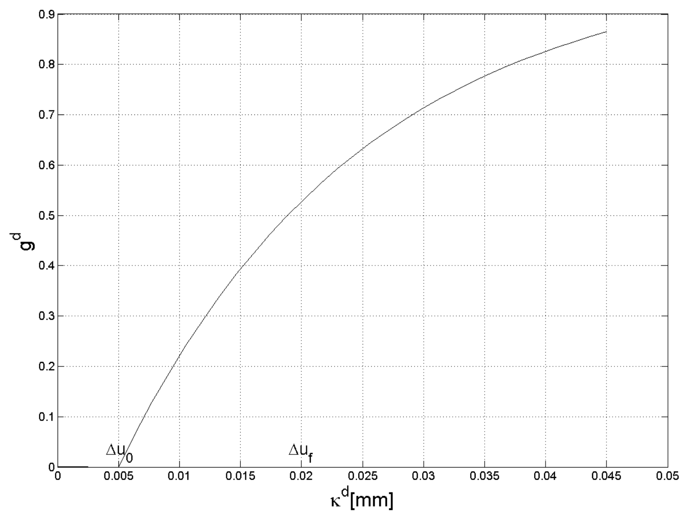

Figure 5. Damage function in cohesion submodel.

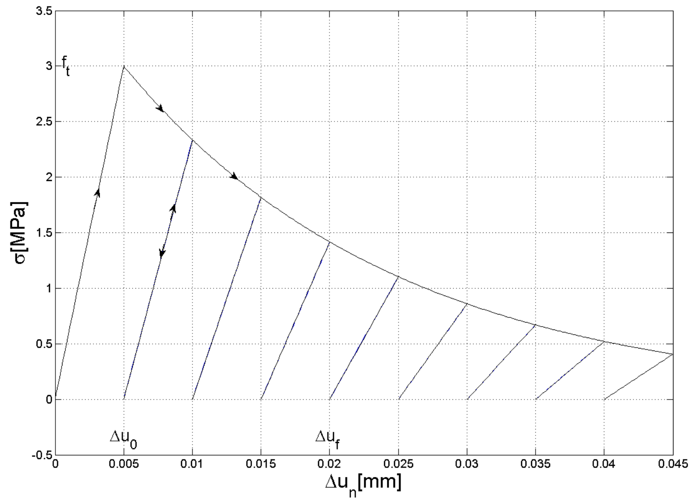

Figure 6. Uniaxial tension with un/reload of cohesion submodel.

Uniaxial tension of the cohesion submodel (and the friction-cohesion model) with un/reload is shown on Figure 6. Also the active material constants appear from the Figure. Stiffness degradation and permanent deformation are exemplified on Figure 6.

4 FRICTION SUBMODEL

When the cohesion is exhausted, friction generated stiffness and strength still remain in the material. These properties are quickly decreasing with increasing crack opening, but as they are increasing with decreasing crack opening, a reversible modelling is relevant. As elaborated below the friction submodel is a non-hardening elastoplastic material with deformation state dependence and an associated flow rule.

In relation to elastic behaviour the above is described by decreasing stiffness with crack opening. Actually is used

$$\begin{bmatrix} d\sigma_f \\ d\tau_f \end{bmatrix} = \rho_e(\Delta u_n)\begin{bmatrix} E_f & 0 \\ 0 & G_f \end{bmatrix}\begin{bmatrix} d\Delta u_n^e \\ d\Delta u_s^e \end{bmatrix} \tag{18}$$

where the deformation state parameter ρ_e is related to the deformations by

$$\rho_e(\Delta u_n) = \begin{cases} 1 & \text{for } \Delta u_n \le 0 \\ \left(\dfrac{1}{1+\dfrac{\Delta u_n}{w_e}} \exp(-\dfrac{\Delta u_n}{w_e}) \right)^{\alpha} & \text{for } \Delta u_n \ge 0 \end{cases} \tag{19}$$

and where Young's modulus E_f and the shear modulus G_f are material constants together with α and w_e in the expression Equation 19 for the deformation state parameter. In order to limit the effective stiffnesses from above to E_f, G_f, the deformation state parameter ρ_e (a stiffness factor) is limited from above to 1.

The plasticity is based on a modified version of the chMC yield function Equation 4. Because the friction submodel is a pure frictional material, the tension strength should vanish. However, theoretically and numerically it is inconvenient that the stress-free state $(\sigma_f, \tau_f) = (0,0)$ correspond to a point on the yield surface. This dilemma is solved choosing the tension strength for the friction submodel f_{tf} to a small positive number. Then f_{tf} is a numerical parameter, not representing a material property.

It is obvious that the frictional behaviour is dependent on the opening of the crack, i.e. completely separated crack faces has no friction capacity and when the crack faces meet again at least some friction capacity re-establishes. As for the elasticity we use a reversible modelling of much the same type. In order to model a reversible strength reduction with the opening Δu_n of the discontinuity surface, deformation state dependence should be incorporated in the yield function. Moreover, the shear deformation Δu_s in the discontinuity surface for moderate compression should initially give expansion in the discontinuity, while for further shear deformation the expansion increase should be smaller ending with zero expansion increase in a pure sliding state. These demands can be modelled in associate plasticity modifying Equation 4 to a closed chMC yield function defined for $-\rho \le \sigma \le f_{tf}$

$$f_f(\sigma_f, \tau_f, \rho) = \tau^2 + \beta|\tau| + \\ + ((c_f - \mu_f f_{tf})^2 - (c_f - \mu_f \sigma)^2)(1+\frac{\sigma}{\rho}) \tag{20}$$

where the deformation state parameter ρ is determined by

$$\rho(\Delta u_n) = \begin{cases} \infty & \text{for } \Delta u_n \le -w \\ \dfrac{\rho_0}{1+\dfrac{\Delta u_n}{w}} \exp(-\dfrac{\Delta u_n}{w}) & \text{for } \Delta u_n > -w \end{cases} \tag{21}$$

and where c_f, μ_f, ρ_0, w are material constants. ρ_0 is the initial value of the deformation state parameter and w the opening scale for strength reduction. Obviously ρ can be interpreted as the deformation state dependent compression yield stress. For enough compression this becomes infinite large reducing Equation 20 to the chMC yield condition. The upper half of the yield surface $f_f(\sigma_f, \tau_f, \rho) = 0$ is shown on Figure 7 for a number of values for the deformation state parameter ρ. The deformation state dependence is shown on Figure 8. Some comments to the yield surface shall now be given.

Consider a stress path with constant normal stress $\sigma = \sigma_P$ and neglect elastic deformations. Increasing the shear stress from 0 gives yield in point A. Obviously the plastic deformations give expansion ($\Delta u_n > 0$), i.e. ρ determined by Equation 21 decreases and then the yield surface shrinks, exemplified by point B, which then represents the new stress point. This process goes on until the plastic expansion ceases, when the stress point reach a top point (a critical state in critical state plasticity vocabulary) of a yield surface - on Figure 7 in point C. Then a stable state has been reached corresponding to well-developed sliding without expansion increase.

The top points for varying ρ correspond obviously to well-developed sliding for varying compression stress. The tangent for $\rho = \rho_0$ to the curve of top points is shown dotted on Figure 7. This situation may be modelled by mC as given by Equation 2. For a compression stress which is not to small, the top points are approximately placed on a straight line, existing knowledge in relation to mC can contribute to the determination of the material constants in the closed chMC yield function. Actually is used $\frac{c_f}{\rho_0} = 0.375$, $\mu_f = 1.30$, which gives a realistic value $\mu = 0.79$ for the friction coefficient in mC.

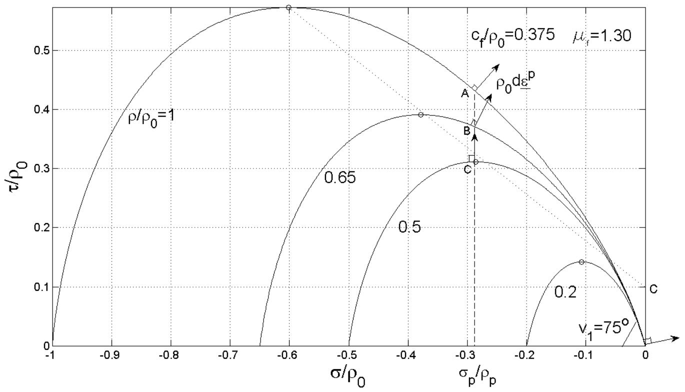

Figure 7. Upper half of deformation state dependent yield surface for friction submodel. $d\boldsymbol{\varepsilon}^p = (d(\Delta u_n^p), d(\Delta u_s^p))$.

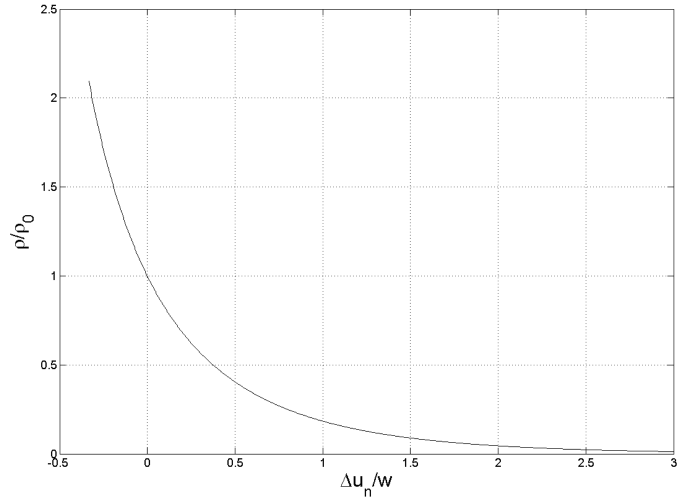

Figure 8. Deformation state dependence of deformation state parameter in yield function for friction submodel.

The half opening angle v_1 of the cusp in the origin of the yield surface is determined from Equation 20 by

$$\tan \mathrm{v}_1 = -\left.\frac{d\tau}{d\sigma}\right|_{\sigma,\tau=f_{tf},0} = \frac{2\mu_f(c_f - \mu_f f_{tf})(1+\frac{f_{tf}}{\rho})}{\beta}$$

$$\rightarrow \frac{2c_f\mu_f}{\beta} \text{ for } f_{tf} \rightarrow 0 \tag{22}$$

Consider a state with the stress point in the cusp point $(\sigma,\tau) = (f_{tf}, 0)$ and a plastic strain increment vector between the yield surface normals in this point. Then the state does not change, i.e. the friction submodel is not activated. Experiments Hassanzadeh (1991) have shown such behaviour down to about v_1 □ 75^0.

5 COMPARISON WITH EXPERIMENTS

The behaviour of the friction-cohesion model has been compared with experimental results Hassanzadeh (1991), where a plane crack is established in a notched specimen. The material constants in the cohesion submodel are

$$E_c = 600MPa/mm, G_c = 250MPa/mm, \mu_c = 0.75,$$
$$c_c = 7.5MPa, f_t = 3MPa, \Delta u_f = 0.02mm,$$
$$\Delta u_0 = 0.005mm$$

and in the friction submodel

$$E_f = 600MPa/mm, G_f = 250MPa/mm, \mu_f = 1.30,$$
$$c_f = 7.5MPa, \beta = 5.22MPa, \rho_0 = 20MPa, \alpha = 1.5,$$
$$w = w_e = 0.15mm$$

The material is first loaded in uniaxial tension to initial cracking for $\sigma = f_t$. This activates only the cohesion submodel of the full material model. Next the material is further loaded in combined tension $d(\Delta u_n)$ and shear $d(\Delta u_s)$ in a constant ratio

$\tan\alpha = \dfrac{d(\Delta u_n)}{d(\Delta u_s)}$. With the given material constants,

for α below about $\alpha = 75^0$ also the frictional submodel is activated. The results obtained with the friction-cohesion model are shown on Figure 9, while the experimental results are shown on Figure 10. Good general agreement has been obtained. The differences for $\alpha = 30^0$ are ascribed secondary cracking in the experiments in accordance with the friction-cohesion model, which indicates that below about $\alpha = 45^0$ Equation 1 is violated.

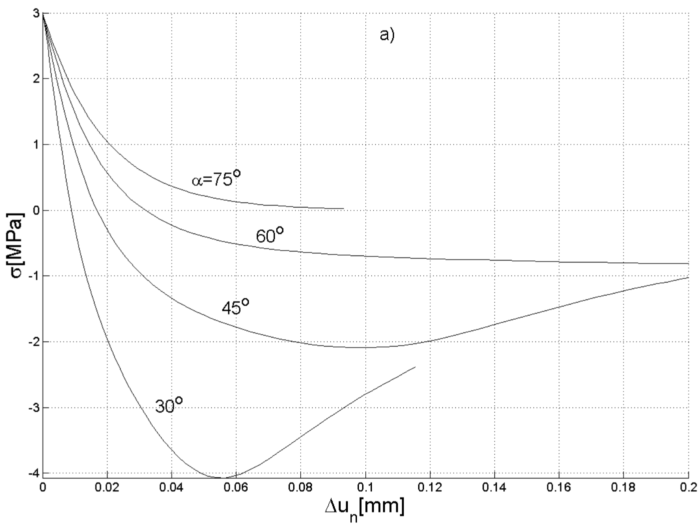

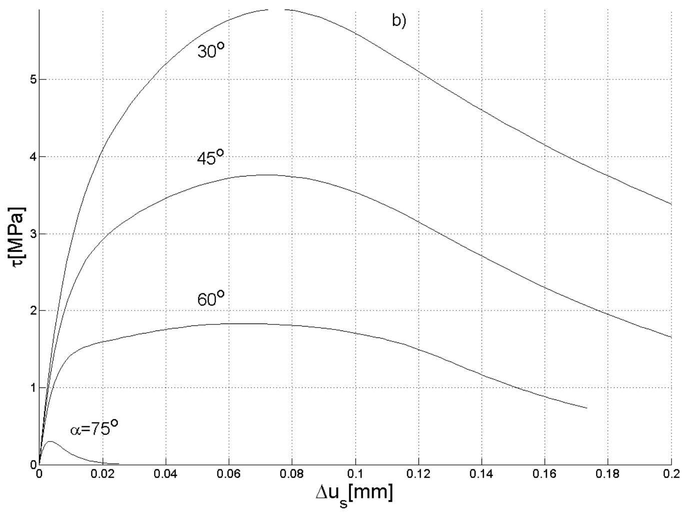

Figure 9. Stresses in friction-cohesion model for some ratios between discontinuity opening and sliding. a) Normal stress as function of discontinuity opening. b) Shear stress as function of discontinuity sliding.

6 CONCLUSION

In the present work a surface constitutive model for cracking concrete has been developed. To achieve accurate results when the crack opens and closes both the cohesion and the friction in the material must be properly modelled. This has led to a two part model with damage of the cohesion with crack deformation and reduced but reversible friction with crack opening. The constitutive model is based on perfect plasticity with deformation state dependence respectively damage in the submodels. The model is in good general agreement with experimental results from Hassanzadeh (1991).

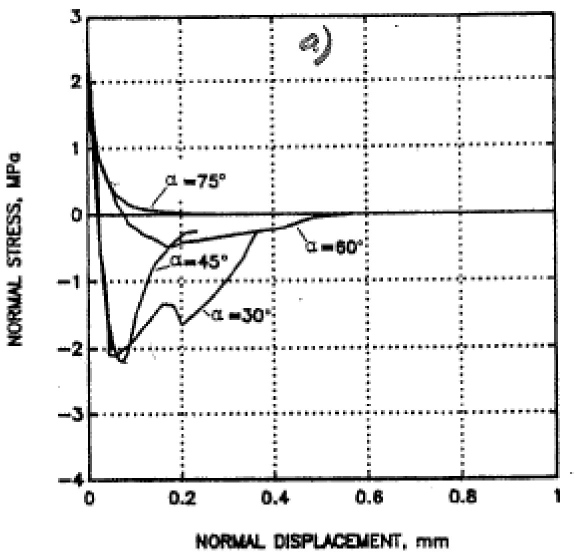

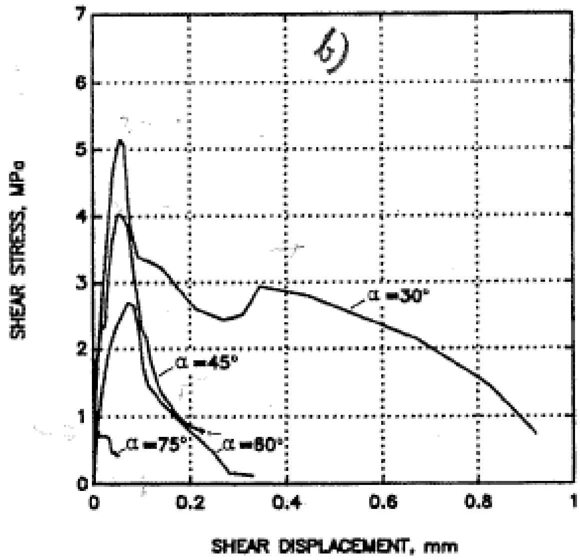

Figure 10. Experimental determined stresses for some ratios between crack opening and sliding Hassanzadeh (1991) a) Normal stress as function of crack opening. b) Shear stress as function of crack sliding.

REFERENCES

Alfano, G. (2006). Combining interface damage and friction in a cohesive-zone model. *Int. J. Numer. Meth. Engrn.* 68:542-582.

Carol, I. (1997). Normal/shear cracking model: Application to discrete crack analysis. *Journal of Engineering Mechanics*, 123(8):765–773, 1997.

Hassanzadeh, M. (1991). Behaviour of fracture process zones in concrete influenced by simultaneously applied normal and shear displacements. Ph.D. thesis, Lund Institute of Technology.

Hillerborg, A. (1989). Analysis of crack formation and crack growth in concrete by means of fracture mechanics and finite elements. *Cement Concrete research 6*, 773–782.

Jefferson, A.D. (1998). Plastic-damage model for interfaces in cementitious materials. *Journal of Engineering Mechanics*, 124(7):775–782.

Nielsen, M.P. (1999). Limit analysis and concrete plasticity, CRC Press.

Spada, A (2009). Damage and plasticity at the interfaces in composite materials and structures. *Comput. Methods Appl. Mech. Engrn.*, 198:3884-3901.